

Development of transformers with natural ester and cellulose or aramid insulation

Ramazan Altay, İrem Hazar, Mahmut Aksoy, Hakan Aktay, Jean-Claude Duart, Radoslaw Szewczyk

Summary — This study describes selected research studies performed for developing design rules for power transformers using natural esters. The presented simulation results verified adequacy of design rules and allowed for adjustments needed for implementing the new insulation system vs. the one based on mineral oil and cellulose-based solid insulation. They were also used as a base for the next transformer design combining natural ester with aramid insulation.

Keywords — Natural ester liquid, electric field distribution, computational fluid dynamics, aramid insulation

I. INTRODUCTION

Modernization of distribution networks increasingly uses transformers utilizing advanced insulation systems based on solid and fluids that have been developed in the recent decades. Taking into accounts new usages of energy, whether they are related to the need for charging electrical vehicles, the integration of renewable energy (wind, solar) or the increase of population in cities leading to higher power demand, it is a constrain that leads to higher stress for electrical equipment like transformers or cables. The manufacturers of such equipment have then to consider evolution of the designs and may need to adopt new materials. Amongst those new materials we can mention about the new generation of core steel with low losses but also new insulation materials that will tend to replace the historical materials being used. This is particularly true in liquid filled transformers where cellulose paper and pressboard combined with mineral oil have been the most common materials used for several decades. The advanced material solutions offer extended lifetime to the insulation system, increased overloadability for the transformers, increased power density, as well as equipment compactness and higher fire resistance or improved sustainability. The last item is mainly related to the usage of natural ester that lowers the carbon footprint as it is biodegradable.

For the solid insulation the most used material is produced in a paper and a pressboard form but made of synthetic fibers. Those fibers were invented in the late 1950's and result from an improvement of the known nylon chemistry. However, a modification of

the nylon molecule with addition of aromatic rings led to the invention of aromatic polyamides, known as aramid fibers. Typical historical applications of aramid-based insulation in liquid filled transformers include on-board traction transformers, wind turbine step-up transformers and transportable mobile transformers for emergency or temporary use. In recent years, aramid insulation has been successfully evaluated and implemented at several distribution system operators (DSOs) in transformers utilizing sustainable peak loading concept or when looking for more grid resiliency [1].

It is also important before looking into a new application to consider design simulations that will help to assess such materials. Some extended work needs to be conducted to understand applicability of the advanced design in such new applications. For example, in wind turbine applications for offshore installations the benefit that advanced materials can have on the design can impact the overall design of the transformers but also the nacelle, where transformers are generally located.

Transformers for solar applications are different from regular transformers in two ways. They can be exposed to a considerable amount of harmonic content due to DC/AC conversion and a typical daily loading cycle that is dependent on the daily sunlight cycle. The daily sunlight can be typically described as a bell-curve as shown in Fig. 1. Both phenomena will have an impact on the temperature rise of the different transformer parts. Two tools have been developed to predict the impact of the harmonics and to take the cyclic daily load into account. A reference transformer of 1600 kVA was evaluated, and different insulation systems have been compared.

For larger power transformers the studies of the electrical field distribution as well as the impact on the cooling from those new materials are important and need to be studied. Adapted numerical model will help to assess the impact on operating temperature inside the transformer while external conditions like ambient temperature must be considered. A 70 MVA transformer design optimization integrating natural esters has been studied.

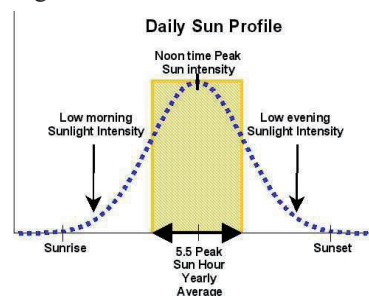


Fig. 1. Example of daily sun profile.

(Corresponding author: Ramazan Altay)

Ramazan Altay, İrem Hazar and Mahmut Aksoy are with the BEST Balıkesir Elektromekanik Sanayi Tesisleri A.S., Balıkesir, Turkey (e-mails: ramazan.altay@besttransformer.com, irem.hazar@besttransformer.com, irem.hazar@besttransformer.com)

Hakan Aktay is with the Opti-Consult, Konak/İzmir, Turkey (e-mail: hakan.aktay@opti-consult.org)

Jean-Claude Duart is with the DuPont Specialty Products Operations Sarl, Geneva, Switzerland (e-mail: JEAN-CLAUDE.DUART@dupont.com)

Radoslaw Szewczyk is with the DuPont Polska Sp. z o.o., Warsaw, Poland (e-mail: radoslaw.szewczyk@dupont.com)

As a second step the design needs to be optimized and the construction parameters as well as the safety margins will need to be chosen for the windings to prepare pilot units to be produced. This is why a study on these construction elements has been carried out. Historical behavior of materials as well as thermal analysis must help to select the proper levels for designing the windings safely.

II. INSULATION SYSTEMS FOR DISTRIBUTION AND POWER TRANSFORMERS

Distribution transformers have a general winding construction which differs from larger power transformers since they operate at lower voltages, generally below 36 kV. However, in recent years we have seen such construction styles to be used in transformers up to 66 kV, particularly in wind turbine transformers. Generally, a distribution winding style uses foil winding in the low voltage coil and layer winding with conductors, round or rectangular, in the high voltage coil as shown in Fig. 2.

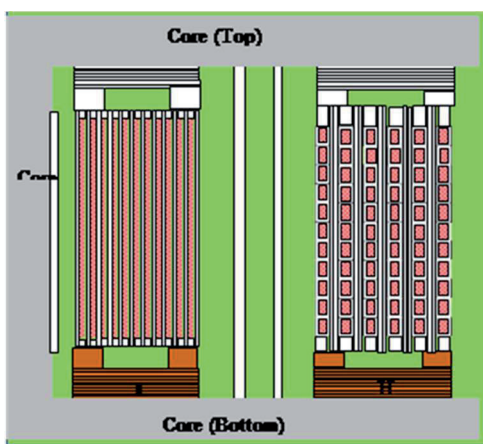


Fig. 2. Example of winding construction for distribution transformers with aramid-based insulation system.

Fig. 3 shows example constructions of various insulation systems for power transformers. Typical arrangement for LV and HV disc windings is shown with different extent of aramid insulation utilized in different winding constructions. In semi-hybrid system, only the conductor insulation uses aramid insulation paper. With this construction the impact of overheating of the windings leading to extensive gassing from the cellulose components in the winding area is limited as aramid degradation is not expected until copper reaches extreme temperatures. In hybrid system, the use of aramid extends from conductor insulation towards pressboard components in vicinity of conductor. But there are still cellulose-based materials used for other insulation components in the winding assembly. Those cellulose-based components together with overheated liquid could give DGA indications on thermal problems within the transformer.

The most insensitive insulation system to higher temperatures resulting from operation or from external factors (like higher power demand or higher ambient temperatures) would be full high temperature insulation systems or “hybrid plus” insulation systems where aramid insulation is combined with ester fluids. In these systems, the use of aramid is most extensive for different insulation parts, and the distance from hot conductors to cellulose components may be significant. In some cases, cellulose components would not be used in the transformer construction at all. In such cases, the liquid may be the only component generating gasses and data useful for conventional transformer diagnostics. However, some work to look for tracers from aramid thermal degradation has

been engaged in recent years leading to better understanding of the ageing protocols [2].

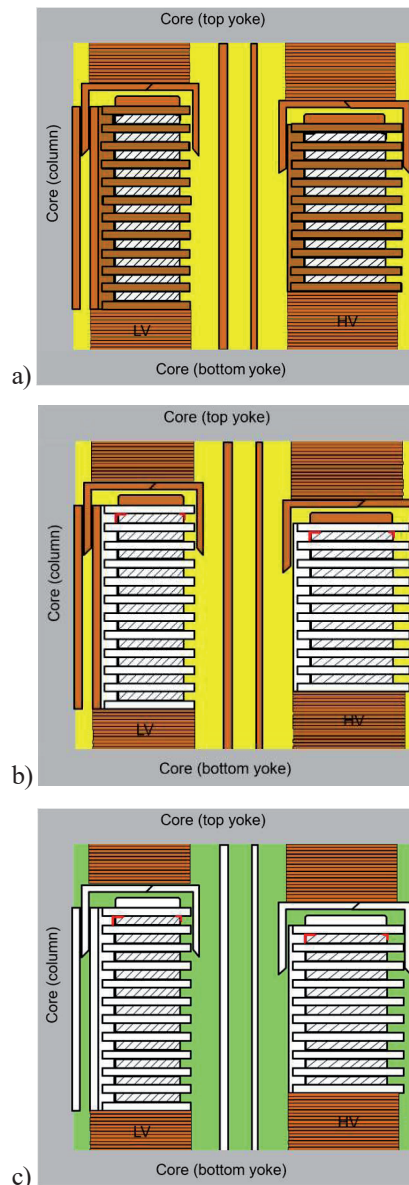


Fig. 3. Example constructions of various insulation systems with aramid: a) semi-hybrid, b) hybrid, c) “hybrid plus” with ester (white color indicates aramid insulation).

III. SIMULATION STUDIES OF VARIOUS TRANSFORMER DESIGNS

The use of advanced design tools has allowed optimization of the transformer design over the years. The work reported in this paper refers to two studies: the first one on a 1600 kVA unit for PV solar application, and the second study has been done on a power transformer 70 MVA integrating natural ester as a cooling and insulating fluid.

A. SIMULATION STUDY OF 1600 kVA SOLAR POWER TRANSFORMER

1. INFLUENCE OF HARMONICS

The current generated by the PV panels is DC and in order to connect the solar plant output to the grid, the current has to be

inverted to AC. The inverted current is far from the ideal sinusoidal shape and thus contains a high level of harmonics. Most of the distribution companies have limits on the amount of harmonics one can connect to their grid (typical 5%, or in Europe even 2.5% total harmonic distortion, THD). One way or the other, the current must be filtered by harmonic filters and that can be done before or after transformation. In large solar power plants there are typically 2 transformations,

e.g. a 100 MVA plant could have 50 units of 2000 kVA going from 400 V to 20 kV and then 1 unit of 100 MVA from 20 kV to 110 kV (or higher). It is cheaper to opt for 1 harmonic filter before the 100 MVA transformer instead of installing 50 filters before each of the 2000 kVA transformers. Let us consider, for the case of argument, that the AC current entering the typical distribution transformer is not filtered. In that case, the transformer manufacturer needs to know the harmonic content of the current entering the transformer. There are 4 ways this information is given to the manufacturer:

1. The customer knows about harmonic problems and overrates the transformer and orders the transformer as such. (In other words, he knows the factor-K.)
2. The customer gives the THD or gives the value of each harmonic in %. In the first case the supplier shall have to convert the THD into a % for each harmonic.
3. The customer gives the K-factor (different from factor-K). The supplier shall then multiply the additional losses with this K-factor, in order to predict the real losses generated in the transformer.
4. The customer has never heard of harmonics. In that case, the manufacturer has to follow a guideline to assume a certain K-factor.

Typically, with no information the transformer should be calculated with a K-factor of 15 [3]. The relation between THD and K-factor will be explained later. To summarize, harmonic content can be translated in a K-factor. This factor is used to multiply the additional losses in the transformer, resulting in higher real load losses and thus resulting in higher temperatures.

2. K-FACTOR/FACTOR-K TOOL

A tool has been developed to calculate the K-factor and factor-K. It is important to understand the difference between the two factors. The K-factor is the factor the transformer manufacturer has to use to multiply the additional losses. That way the real losses and temperature can be estimated. The factor-K is a factor by which one can derate or upgrade a transformer to cope with the harmonic content or to give an equivalent sinusoidal rate. Table I provides an example of a harmonic spectrum till the 25th harmonic that will be used of the optimization of the 1600 kVA design (cellulose, mineral oil).

TABLE I
PERCENTUAL PART OF NTH HARMONIC IN NOMINAL CURRENT

harmonic	I_h (%) $I_n \% I_{nom}$
1	86.12693
3	36.58379
5	21.95027
7	15.67877
9	12.19460
11	9.97740
13	8.44241
15	7.31676

17	6.45596
19	5.77639
21	5.22626
23	4.77180
25	4.39005
I_{nom}	100.0

Using industry experience [4] and the example of the harmonic spectrum, the tool allows to derive a THD value of 0.59 corresponding to the same harmonic content as indicated in the Table II.

TABLE II
OUTPUT EXAMPLE OF THE CALCULATION TOOL

thd	0.59		
alfa	thd/0.463		1.27429806
i1	$(1/1+thd^2)^{0.5}$	1	86.1269258
ix	alfaix/x	3	36.5837914
		5	21.9502748
		7	15.6787677
		9	12.1945971
		11	9.97739764
		13	8.44241339
		15	7.31675827
		17	6.45596318
		19	5.77638811
		21	5.22625591
		23	4.77179887
		25	4.39005496

Then the tool calculates the K-factor which is in this case 15.1962. For deriving the factor-K, we need transformer losses values as show in Table III.

TABLE III.
1600 KVA TRANSFORMER LOSSES

Calculated additional losses HV [W]	617
Calculated additional losses LV [W]	262
DC losses HV [W]	8280
DC losses LV [W]	5427
DC losses leads [W]	410
Additional losses outside windings [W]	318
Additional losses/ DC losses [%]	8.5

The resulting factor-K is then calculated together with the derating factor. Values are reported in Table IV.

TABLE IV
DERATING FACTOR AND FACTOR-K FOR 1600 KVA TRANSFORMER

Derating-factor with harmonic content	0.862
Factor-K to determine equivalent sinusoidal load	1.160

The interpretation of this information is the following: If the 1600 kVA transformer is loaded with this harmonic content

as described in the example, the transformer can be loaded with maximum 1380 kVA to avoid overheated and accelerated degradation of the insulation system based on cellulose. On the other hand, if the nameplate of the transformer indicates 1600 kVA with K-factor 15 explicitly mentioned, the transformer could be loaded with a sinusoidal load of 1856 kVA.

3. INFLUENCE OF LOAD CYCLES

It is trivial, that output of PV cells follows the cycle of the daylight. During the night we can assume that only no-load- losses will be present. During the day the output follows the cycle of the sun. This results in a bell-shape load profile. In the theoretical profile, and assuming a daily 12 h daylight, sigma of the bell curve is 2 h resulting in 68% of the daily energy being concentrated in a period of 4 h (the +/-3 sigma being the 12 h daylight is then theoretically 99.7% of the daylight). The load will result in losses that in their turn result in temperature variations. The goal of the study is to investigate whether it is possible to design an ideal cooling structure that can cope with those loads. Aging of insulation material and general safety limits must be evaluated and compared for different insulation/cooling systems. Intuitively we can already see that larger units (with important time-constants) could probably be overloaded. By the time the transformer reaches critical temperatures, the load is already going down. There are some guidelines to come up with dynamic temperature calculations. However, these analytical formulas are not sufficient to describe the models we are investigating. Therefore, a new calculation tool was created and will be describe further.

4. LOAD CYCLE TOOL

The model is based on a 4-body mass heat exchange. The original theoretical model was a 3-body mass heat exchange solved analytically [5]. In this study the model was expended to 4-body mass and the problem (system of four ordinary differential equations) was solved by the numerical method Runge-Kutta 4th order.

The four bodies in our system are: core, LV winding, HV winding and oil-tank while originally LV and HV windings were treated as one single body. The steady state temperature rises are considered for core, LV and HV, the rise over the average oil temperature. Specific heat for the different materials is filled in with the values from original model. In what follows, the specific heat for aramid and ester oil were kept with the same value as for cellulose and mineral oil. Load is then input in the calculation tool for the 1600 kVA, and it is assumed a cold start and a load of continuous 100%, which then results in the following temperature rises as shown in Fig. 4.

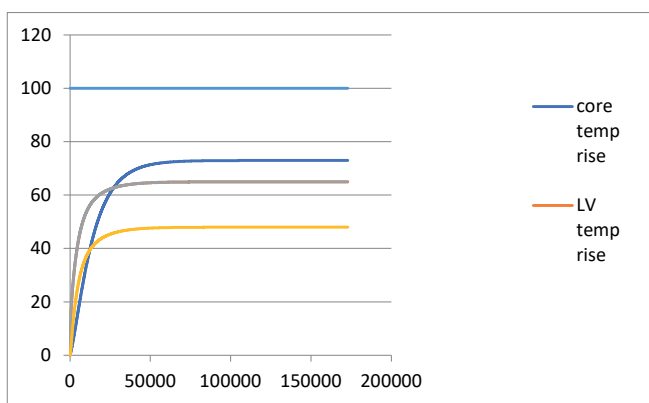


Fig. 4. Temperature rise for 1600 kVA transformer.

We can see that after around 50000 seconds (14 h) the transformer reaches steady state conditions. 73°C for core, 65°C for LV and HV, 48°C for average oil (48 / 0.8 = 60). This is trivial because our model is based on the calculated steady state values. All temperatures are temperature rises over ambient.

5. EVALUATION OF REFERENCE 1600 kVA TRANSFORMER

As a first exercise we are going to evaluate what is happening with the temperatures with a typical loading cycle. Then we are going to look at what possibilities there are with regard to overload when we replace the insulation materials and the oil. We are assuming daylight between 7 AM and 7 PM, if we apply the Bell-curve model then we can generate a load profile with the equation (1):

$$load\ pu = \frac{1}{\sigma \cdot \sqrt{2\pi}} * e^{-\frac{(x-\mu)^2}{2 \cdot \sigma^2}} \quad (1)$$

Where μ is the average time between 7 AM and 7 PM, 13.5 and σ is the standard deviation of 2 h. This gives a per unit graph were the total surface under the curve is 1. In order to translate this in % load we have to divide by the maximum value (at 13.5 h) and multiply by 100. For the reference transformer, this results in the following 2 days cycle as shown in Fig. 5, assuming cold start at midnight of the first day, and only no-load losses till 7 AM are show in Table V.

TABLE V

CALCULATED VALUES FOR TEMPERATURE RISES IN 1600 KVA TRANSFORMER

	Core rise	LV rise	HV rise
	50.43386539	50.99716039	51.01126495
Gradient max	14.52883171	Average oil rise	36.48243324
Hot-spot rise	61.58475643	Top oil rise	45.60304155

In this case we see that the temperatures are far under what is allowed by standards (60/65/78°C) as we only reach 46/51/62°C for the top oil rise, average winding rise and hot spot rise.

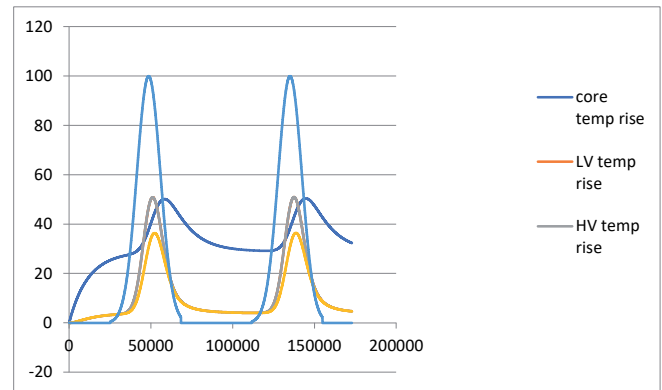


Fig. 5. Temperature rise, 2-day cycle for 1600 kVA transformer.

An overload factor is then applied. The goal is to see how much peak load we can apply and still be safe with regards to temperature. We are going to evaluate the existing design with two insulation systems: a mineral oil/cellulose system and aramid/synthetic ester system. This means in a first step, there is no evaluation of an optimized transformer with different insulation material. This will be done in a next stage.

TABLE VI

TEMPERATURE RISE FOR NO OVERLOAD AND SHORT TERM OVERLOAD CONDITIONS

	No overload				Short term overload		
	Winding rise	Top oil rise	Hotspot rise	Overload factor	Top oil rise	Hotspot rise	Overload factor
Mineral oil / cellulose	64	57	77	1.13	74	102	1.31
Synthetic ester / aramid	102	89	122	1.44	99	136	1.52

The Table VI shows the possible overload if we replace in the existing design the insulation and/or oil. The values in yellow are the limiting values. The existing design can have a peak load of 1.13 times 1600 kVA. With the existing load cycle, the temperatures would still be safe. If we would have filled the transformer with synthetic ester and insulated with aramid paper and board, we could load the transformer with a peak load of 1.44x1600. Similarly, we can apply the short-term overload criteria for evaluating the maximal peak load. It has to be stressed that just replacing the insulation structure and the oil is not really an optimal design. Basically, this means at this moment that the optimal 1600 kVA (mineral oil / cellulose) transformer can be overloaded with no ageing with a factor 1.13. The non-optimal synthetic ester / aramid can be overloaded with a factor 1.44. It also needs to be mentioned that the short-term overload situation results in considerable ageing in the case of mineral oil / cellulose, while in the ester / aramid combination there is still no aging. In a next step we need to evaluate optimal designs of every insulation combination.

6. COMPARISON OF OPTIMAL DESIGNS

The 1600 kVA transformer with different insulation structures is then optimized and the possible overload factor for a derated transformer that would have the same losses and impedance as the 1600 kVA is used. The initial transformer mineral oil-cellulose is already designed. In the Table VI, we saw that this transformer could be overloaded by a factor 1.13 without ageing and with a factor 1.31 if we allow short term overload temperatures. The overload factor without aging leads to the following calculation deriving the optimized design of 1400 kVA.

$1600 / 1.13 = 1416$, we round to the nearest 50 kVA so we optimize the design to 1400 kVA. While an optimize design with allowed short term overload will lead to a different optimized design of 1200 kVA. Then, the maximum temperature rises are derived from the calculation tool once using the design data of the transformer with a peak load of 1600 kVA. In the Table VII, the two combinations considered and allowed temperature rises are shown (ambient is considered maximum 40°C).

TABLE VII

TEMPERATURE RISE LIMITS FOR NO OVERLOAD AND SHORT-TERM OVERLOAD CONDITIONS

Insulation structure	No overload			Short-time overload	
	top oil	winding	hotspot	top oil	hotspot
Mineral oil / cellulose	60	65	78	75	120
Synthetic ester / aramid	90	125	150	100	180

After optimizing the two combinations at 1600 kVA, the temperatures were derived, applying the design in the load cycle calculator. Then overload factors were found (one for no aging and one for short term overload.) The resulting transformer ratings and their temperatures are depicted below. The temperature results shown in

Table VIII are all based on a load of 1600 KVA.

TABLE VIII

TEMPERATURE LIMITS FOR SIMULATED RATINGS TO 1600 KVA

	Top oil	Winding	Hotspot
1600 kVA-60-65-78	46	51	62
1400 kVA-60-65-78	55	62	75
1200 kVA-60-65-78	66		94
1600 kVA-90-125-150	62	95	111
1400 kVA-90-125-150	74	108	127
1250 kVA-90-125-150	85		139

For example, a 1250 kVA-90-125-150 is a synthetic ester / aramid design, if loaded with a peak load of 1600 kVA and with the assumed bell-curve load, top oil would rise 85°C and hotspot would have a rise of 139°C (well below allowed limits). The values shown in bold are the values higher than what would be allowed for continuous condition. A mineral oil / cellulose design transformer 1200 kVA loaded at 1600 kVA would be reaching temperatures that would degrade dramatically the insulation system.

B. SIMULATION STUDY OF 70 MVA POWER TRANSFORMER

In this study, electric field intensity distribution of 70MVA, 36/12 kV power transformer with natural ester and cellulose was investigated in ANSYS Maxwell V2022 R2 and the thermal effect of natural ester oil on the windings was investigated in ANSYS FLUENT V2022 R2. The three main dielectrics used in transformer insulation are: transformer oil, paperboard barrier, oil-impregnated paper. The relative permittivity is shown in Table IX.

TABLE IX

DIELECTRIC PROPERTIES IN FUNCTION OF TEMPERATURE

Temperature	Relative permittivity		
	25°C	90°C	130°C
Natural ester	3,3	3,0	2,9
Low density pressboard	4,4	4,4	4,5
High density pressboard	4,6	4,8	5,2

The assumptions made during the analysis are that the LV, HV and TAP windings are considered as a single cylinder with axisymmetric uniform tension. Conductors are rounded to a radius of 0.5 mm by rounding from the corners and

0.5 mm paper coating is given. The boundary condition taken for this finite element problem is the Dirichlet boundary condition. The limb, yoke and core are considered as the boundary and grounded. The transformer is subject to three main high voltage tests:

1. lightning impulse test,
2. short duration power frequency test,
3. long duration power frequency test.

This equivalent voltage level is referred to as the design insulation level (DIL) expressed in kV_{rms}. Thus, there is only one DIL inside the transformer at any one time, with maximum equivalent one minute power frequency voltage levels for four different tests. It is important to convert all these values to one minute power frequency test. The highest of these values is used as excitation for the HV winding during simulation. As shown in Table X, design insulation factors are taken for historical conversion factors. [6] Tables X and XIII for medium voltage transformers below 75 kV indicate that it can be assumed that the DIL used for mineral oil can also be used for esters.

TABLE X
DESIGN INSULATION FACTORS

Condition	DIL Factor
Lightning impulse	2,3
AC one-minute test level	1,0
AC one-hour test	0,8

This section presents the description of the numerical model that allow us to study the thermal phenomena that occur in the analysis platform. This model has been carried out using the ANSYS FLUENT 2022 software. Thereby, the governing equations and the boundary conditions of the fluid study applied to 2D section of the winding are used. Also, computational domain, meshing and material properties are shown. Winding loss outputs are used as inputs for thermal analysis. While evaluating the losses, I²R+Eddy losses were evaluated homogeneously as total losses. The loss values used are as follows in Table XI.

TABLE XI
LOSS VALUES

75°C	I ² R (kW)	Eddy Loss (kW)
LV Winding	100	5,5
HV Winding	141	12,2

Many properties of ester oils, such as viscosity, conductivity, and thermal capacity, differ from mineral oils. Table XII details some of those properties.

TABLE XII
FLUID PROPERTIES

	Mineral Oil	Ester Fluid
Flash Point (°C)	110–175	250-310
Fire Point (°C)	110-185	300-322
Kinematic Viscosity (cSt) (90°C)	2,3	7-8
Density (kg/dm ³) (20°C)	0,83-0,89	0,9-1,0

Due to installation of the transformers in southern region of Turkey, it was critical to consider impact of higher ambient temperatures. The annual temperature distribution of this region is examined, and thermal analyses are completed according to the climate conditions in that specific area of Turkey. The results of the simulation should present the changes with different ambient temperature considerations. The finite volume-based numerical method solves the Navier–Stokes equations, which state the conservation of mass, momentum and energy for a fluid flow. For an incompressible fluid (oils can be considered this way), the equations that state mass, momentum, and energy conservation are equations (2), (3) and

(4). On the other hand, for the solid domain, the equation that state energy conservation are:

$$\nabla \cdot (\rho u) = 0 \quad (2)$$

$$(u \cdot \nabla) \rho u = -\nabla p + \mu (\nabla^2 u) + g \rho \quad (3)$$

$$\nabla \cdot (\rho C_p u T) = \nabla \cdot (k \nabla T) + q_s \quad (4)$$

$$0 = \nabla \cdot (k \cdot \nabla T) + q_s \quad (5)$$

Where ρ , ρ_{ref} , u , p , μ , g , C_p , T , k , and q_s of equations (2), (3), (4) and (5) are density, density of reference, velocity vector, pressure, dynamic viscosity, gravity, specific heat capacity, temperature, thermal conductivity, and heat source, respectively. The right-hand terms of (3) are the pressure force, the viscous force, and the buoyancy force, respectively. The latter represents the force that drives the flow in natural convection regime, and it is related to density gradients in the fluid. This equation helps to represent the natural convection effect in computational fluid dynamics.

IV. DEVELOPMENT OF ADVANCED TRANSFORMERS

Integrating new materials in a design is always challenging as new applications require validation. The 70 MVA,

36/12 kV power transformer design is chosen for design optimization. The insulation structure in 70 MVA power transformer is showed in Fig.6.

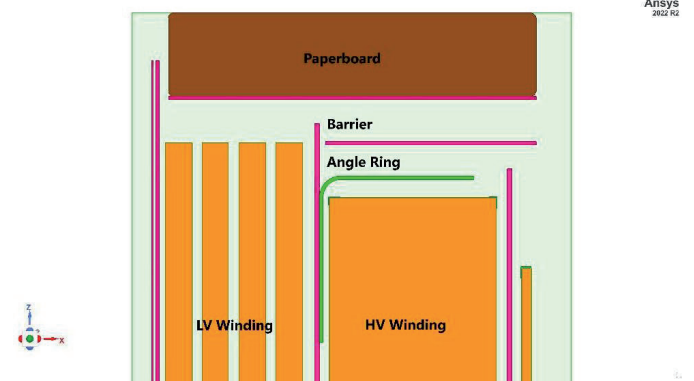


Fig. 6. Insulation structure of 70 MVA transformer.

The potentials of transformer core, tank and LV windings are defined as 0 kV, thereby regarded as grounded during the 1 min induced voltage test. Voltage is applied to the HV winding at the rate of the Design Insulation Level (DIL) coefficient. Safety factors are calculated by means of DIL factor for BIL. These are based on attached graph “DIL Factor” (from document “AC Insulation Design...” [7]) and can be derived by the equation (6):

$$\text{BIL Factor} = \text{BIL} / \text{AC} \Rightarrow 2.3 \quad (6)$$

TABLE XIII
FACTORS FOR CONVERSION TO ONE MINUTE (RMS) POWER FREQUENCY LEVEL

Test voltage	Multiplication factor
Lightning Impulse Level (BIL)	$\sim (1/2.30)=0.44$
Switching Impulse Level (SIL)	$\sim (1/2.80)=0.55$
Long Duration (one hour) Power Frequency Voltage	$\sim (1/0.80)=1.25$

After calculation of DIL for 70 MVA, the transformer the one-minute power frequency voltage 73.913 kV is taken as excitation for calculating. Finite element electric field analysis is performed using the aforementioned boundary conditions at the main insulations for the design. Then, voltage and electric field distribution plots are shown in Fig. 7 and Fig. 8.

Historical limit curves shown in Fig. 9 are used for the AC analysis. When we inspect the reference table, A41-5 limit curve is indicating the protection level due to isolation paper and A41-6 limit curve is indicating the protection level due to barriers. We are using the A41-6 limit curve as this is the safer protection level.

Safety margins in windings middle part (HV-LV) for 1 minute dielectric AC test are listed below. These margins are obtained by comparing calculated values by Finite Element analysis with the historical oil breakdown curve. These margins are obtained by comparing calculated values (red colored) of FEM analysis with the Weidmann oil breakdown curves (black colored). For oil duct numbering, please follow the direction on red colored streamlines. The main principle for oil duct numbering is that the direction of arrows is always from higher potential to lower potential. It means that direction is from right to left between HV/LV windings. Additionally, stress values on oil duct between HV and LV winding are obtained from Fig. 10 (red colored). The analysis results are below the current values and in the safe zone:

Oil Duct 1 - 65,25 % safety factor,
 Oil Duct 2 - 61,14 % safety factor.

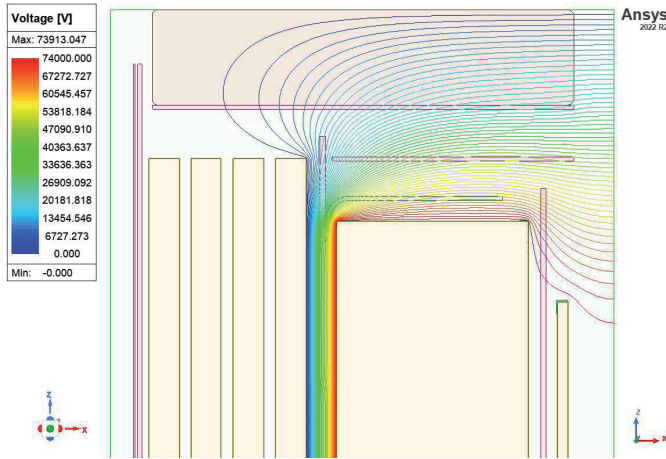


Fig. 7. Voltage distribution.

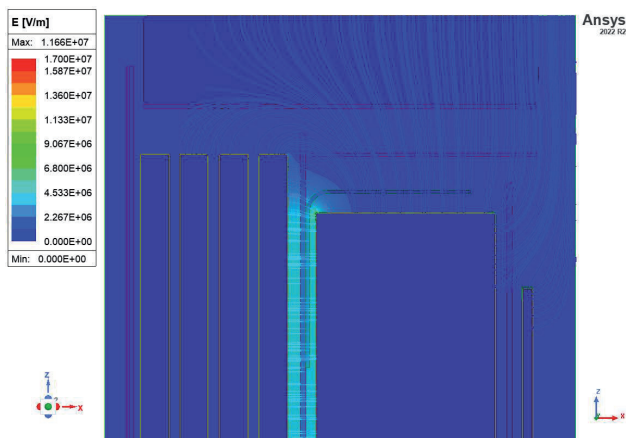


Fig. 8. Electrical field distribution.

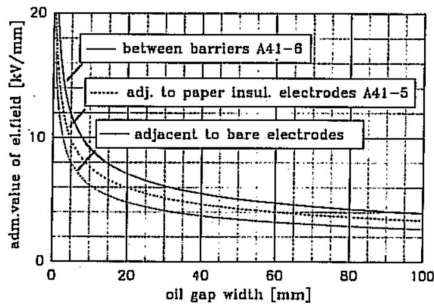


Fig. 9. Historical field distribution limits.

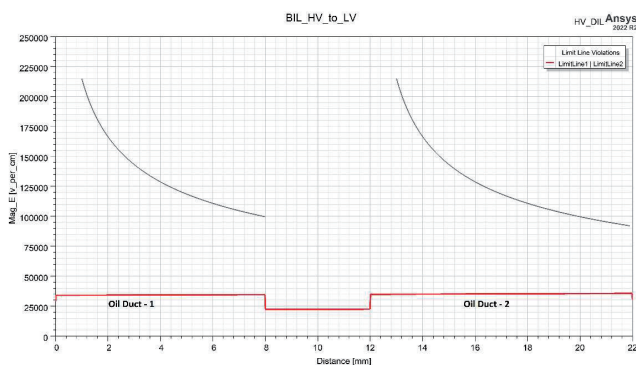


Fig. 10. Oil stress distribution and safety factors between HV winding and LV winding.

Thermal analysis was made separately according to mineral oil and ester liquid, the ambient temperature of 20°C and 40°C in order to see the effect of different ambient temperatures and different liquids. In each case, the maximum temperature is on the 1st layer of the LV winding. In the worst case of ester, the maximum gradient is 29 K for LV winding and 26 K for HV winding. Average gradients were obtained as 19 K for LV winding and 15 K for HV winding in the ester case. Within the scope of the project, the hot spot was also examined. For the 70 MVA LV winding, the hot spot was clearly visible on the first layer. The 70 MVA HV winding was also located on the first layer, but the 2nd, 3rd, 4th and 5th were also close to hot spot temperatures. The LV winding hot-spot value is about 8 K higher than the HV winding hot-spot value. The 70 MVA power transformer with ester CFD analysis results are shown in Table XIV. Table XV shows the mass flow distribution between the LV winding and HV winding.

TABLE XIV
 CFD RESULTS FOR 70 MVA TRANSFORMER

		Average gradient (K)	
		LV	HV
Ambient Temp °C	20	19,25	15,25
	40	14,81	12,01

TABLE XV
 MASS FLOW DISTRIBUTION RESULTS FOR 70 MVA TRANSFORMER

	LV	HV
Mass flow (% kg/s)	36	64

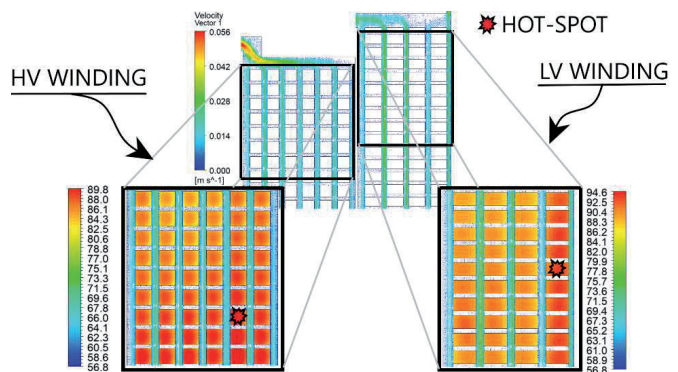


Fig. 11. Hot spot locations.

The comparison of different liquids has also been carried out in scope of this project. Due to lower viscosity advantages of mineral oils, the hot spot and average temperature results were better in mineral oil case. Average temperature rise and hot-spot were higher by 3 K and 6 K respectively, due to the use of the ester liquid instead of mineral oil in the LV winding CFD simulation model. The region with the maximum temperature increase (worst-case) is seen on the 1st layer of the LV winding. The hot spot location is expected in 75 mm below from 1st layer of the LV winding and 110 mm below from 2nd layer of the HV winding as shown in Fig. 11.

V. CONCLUSION

The work conducted on the development of advanced transformers with alternative insulation systems required a thorough analysis on how these materials can be integrated in the design. Whether we consider small distribution transformers (below 10

MVA, below 66 kV) or larger power transformers, studies are required to allow for an optimized use of such materials. Studies show that integrating such material can provide significant benefits in terms high loading capabilities without loss of life for transformers in PV solar installations or improve environmentally the large power transformers.

REFERENCES

- [1] R. Szewczyk et al., "Design of innovative resilient transformers for maximum operating flexibility", *CIGRE Session 2022*, Paper A2-11022
- [2] R. Szewczyk et al., "Thermal faults simulation for aramid insulation in liquid immersed power transformers", *CIGRE Session 2022*, Paper D1- 11027
- [3] J. Leung et al., "Solar power plant harmonic emission – design and commissioning case study", *Solar Integration Workshop*, Dublin, Ireland, 2019
- [4] "Loading transformers with non-sinusoidal currents, ABB, Doc. 1LES100070-ZB, rev. 1, 2007
- [5] K. Karsai et al., "Large power Transformers", Elsevier, 1987
- [6] S. V. Kulkarni, S. A. Khaparde, "Transformer engineering: design, technology and diagnostics", CRC press, 2017
- [7] D. J. Tschudi, "AC insulation design: paper-oil insulation systems", WICOR Insulation Conference, Rapperswil, Switzerland, 1996